HOT SPOT RISK ANALYSIS ON SILICON CELL MODULES

Stefan Wendlandt[1,3], Alexander Drobisch[1], Torfinn Buseth[2], Stefan Krauter[1,3,4] and Paul Grunow[1]
[1] Photovoltaik Institut Berlin AG, Wrangelstr. 100, D-10977 Berlin, Germany
Phone: +49 (30) 814 52 64 0, Fax: +49 (30) 814 52 64 101, e-mail: wendlandt@pi-berlin.com
[2] Elkem Solar AS, P.O. Box 8040 Vaagsbygd, NO 4675 Kristiansand, Norway
Phone: +47 3801 7399, e-mail; torfinn.buseth@elkem.no
[3] Technical University of Berlin, Department of Energy and Automation Technology, Einsteinufer 11, D-10587 Berlin, Germany, e-mail: krauter@iee.tu-berlin.de
[4] University of Paderborn, Faculty of Electrical Engineering, Informatics and Mathematics, Institute for Sustainable Energy Concepts, Pohlweg 55, D-33098 Paderborn, Germany, e-mail: krauter@nek.upb.de

ABSTRACT: The hot spot risk of crystalline silicon modules is the only reliability and safety issue, which is attributed to cell properties. The increased hot spot risk results from local shunts or deformations of the *pn*-junction, which might origin from inhomogeneities in the raw material of the waver or bad cell processing. This paper presents an overview of existing and new approaches for the hot spot analysis of crystalline silicon cells. Its aim is to provide a reliable, non-destructive and fast testing-scheme, that can be used for screening of large lots of finished modules or as a final test in the module production. Infrared-thermographs and dark-current measurements are used to forecast the probability of a destructive hot spot effect deriving from partial shading in the field. A new hardware set-up is proposed and its feasibility for an in-line production use is discussed. Finally, the ongoing discussion between different national reliability standards for the hot spot endurance test is commented.

KEYWORDS: hot spot, crystalline silicon cells, reliability

1 INTRODUCTION

On the way to electrical grid parity of PV systems, PV installation density increases, and more systems suffer from shadowing along with the related hot spot risk. Typical shading situations of PV modules are resulting from self-shading of adjacent modules, antennas, bird droppings, smokestacks, trees and/or from building services engineering. Such shadowing example is shown in Figure 1.

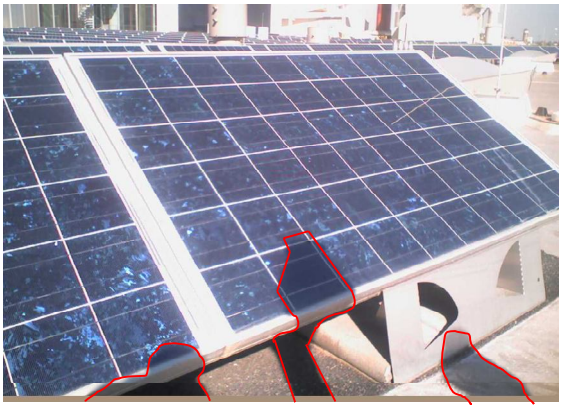

Figure 1: A multi-c-Si PV module which is shaded (red outline) from building services engineering.

By the classification of shadowing types it has been shown that smaller, but fully opaque shadows are the most critical ones. Next to the shadowing type the hot spot risk of modules depends also from the climatic conditions such as the ambient temperature (worst case: *high*), the irradiance (worst case: *high*) and the wind speed (worst case: *low*). Furthermore the module installation situation is also a risk factor concerning the hot spot risk (worst case: *building/roof integrated without or with little backside ventilation*).

However, the highest hot spot risk is given by the wafer raw material, the process quality in the solar cell production, the string length in a given module design and the cell sorting. Since a long time the hot spot effect has been investigated by several research groups. The studies focused on the empirical description of *IV* curves in reverse bias [1], the hot spot risk due to cell mismatching in a module [2], the analysis and detection of hot spots in single cells [3] [4], and hot spot investigations at the PV module [5] [6] [7] [8] [9].

To determinate the hot spot susceptibility, indoor tests are most effective. An indoor hot spot test is part of the standard IEC 61215:2005 Ed.2 product qualification and type approval of crystalline silicon PV modules. This test is divided into two parts: at first, the highest-risk-cell (or worst case cell) has to be identified by fully shading each cell in a solar simulator and choose the cell with the highest leakage current. In most cases this cell shows indeed the highest rise in temperature. An example of a multi-c-Si module with three 20-cell-strings and different total shaded cells is shown in Fig. 2.

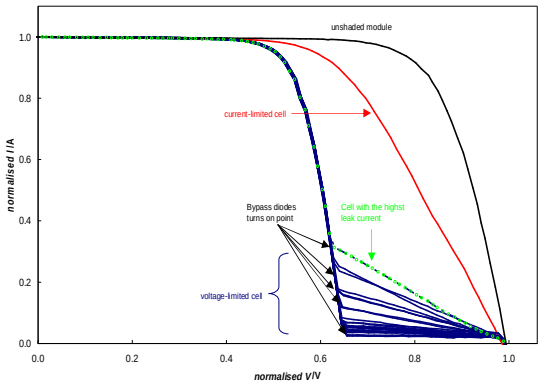

Figure 2: The shaded cell is reversed bias by the un-shaded cells. Bypass diodes are used to reduce the reverse bias voltage and with this the power dissipation.

Figure 2 shows that two different kinds of reverse bias cells can be measured under our flash simulator Pasan SS3b: the current-limited (red line) or voltage-limited (blue lines) ones. The current-limited ones are considered to be less critical in the corresponding standard IEC 61215:2005 Edition 2.

In the second step of the hot spot test the module has to be irradiated in a steady-state solar simulator (minimum: class C) for five hours (home-made simulator with HQI lamps). Following the procedure from the IEC standard, the worst case cell is first fully and then partly shaded to adjust to maximum energy dissipation in the shaded cell from absorbed light and reverse biasing.
Because of the absence of hot spot in-line detection in actual production lines for wafers, cells or modules, each manufactured module introduces an unknown hot spot risk in the field. Therefore, fast hot spot detection methods for modules and their accessible risk parameters are evaluated in this work.

2 EXPERIMENTAL SET-UP & TECHNICAL DESCRIPTION

2.1 ELECTRICAL ANALYSIS

The first method is the hot spot analysis by fitting the dark condition, reverse *IV* curve to the Bishop model [10]. To measure the dark curve of the single cells the bypass diodes have to be removed from the module. The complete module is then exposed to the sun simulator with only one cell shaded at a time. These illuminated IV curves with partly shading are similar as shown in Fig. 2, but with out the turn on (break point) of the bypass diodes. They are fitted to calculated curves according to Bishop's model. The dark current is given by:

$$I = \underbrace{I_{ph} - I_0\left[\exp\left(\frac{V+IR_s}{nV_T}\right)-1\right] - \frac{V+IR_s}{R_p} - I}_{forwards-bias-range} \qquad (1)$$

$$\underbrace{-a\frac{V+IR_s}{R_p}\left(1-\frac{V+IR_s}{V_{break}}\right)^{-n}}_{reverse-bias-range}$$

The Bishop model consists of the one-diode model and the extension term which describes the reverse bias range of the *IV* curve. The relevant parameters for the hot spot risk are: the breakdown voltage V_{break}, the shunt resistance R_p and the avalanche exponent n.

The Bishop model has been chosen over other models, because it reveals good matching with the experimental curves. For the reverse current regime under investigation here, the multi diode models are not offering any additional benefit. An example for such a curve fit for a reverse-bias cell (encapsulated in a module, totally shaded), following Bishop and including fit error considerations, is shown in Fig. 3.

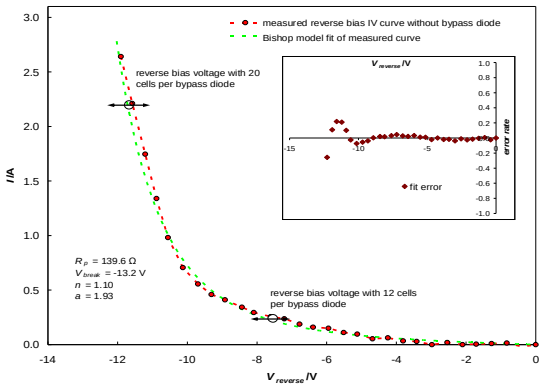

Figure 3: The reverse-bias *IV* curve (without a bypass diode) can be described well by the Bishop model.

Fig. 3 also indicates the ranges in which the bypass diode turns "on" - for two cell strings of different length. These ranges have been determined during the search for the highest-risk-cell in the procedure from the IEC standard

2.2 THERMAL ANALYSIS

Next to the electrical analysis a (electrical)-thermal one will be proposed. The thermal investigation is interesting because it lumps the hot-spot-risk factors together, i.e. the temperature and the spot size. A new parameter is introduced: the leakage current density $J_{leakage,}$ which is defined as follows:

$$J_{leakage} = \frac{I_{leakage}}{A_{hot-spot}} \qquad (2)$$

To determinate the leakage current density, the leakage current $I_{leakage}$ and the size of the hot spot $A_{hot-spot}$ have to be known. $I_{leakage}$ can be measured as described in (1) and shown in Fig. 2. The information about the actual area $A_{hot-spot}$ can be obtained from an infrared image, the camera sensor pixel size, and the optical distances between the image and the object.

Regarding test performance and equipment, this approach is equal to the test described in the IEC standard. The module has to be placed in a steady-state solar simulator and irradiated with an irradiance of E_e = 1,000 W/m². Thereby the cell to be tested has to be fully shaded.

After a defined time of 60 sec, an infrared image of the tested cell is taken: The image gives information about the temperature increase, the affected area, and its location. For the infrared image an *IR* camera with a resolution of 320 x 240 pixels and a thermal sensibility of 0.10 K at 30°C has been used. The distance between object and camera is fixed at 0.66 m.

3 RESULTS

3.1 ELECTRICAL ANALYSIS

For the dark reverse curve analysis of single cells in a complete module, seven modules with five strings consisting of 12 156 mm x 156 mm cells in series per by-pass diode were used. Fig. 4 shows V_{break} and R_p as a function of the dissipated power P_{loss} (at a reverse voltage of V = -10 V). The applied reverse voltage of V = -10 V has been chosen because that value is most commonly used in the PV industry, although in the present case with 12 cells a value of V = -7 V (= 12 x 0.5 V + 1 V) would already be adequate.

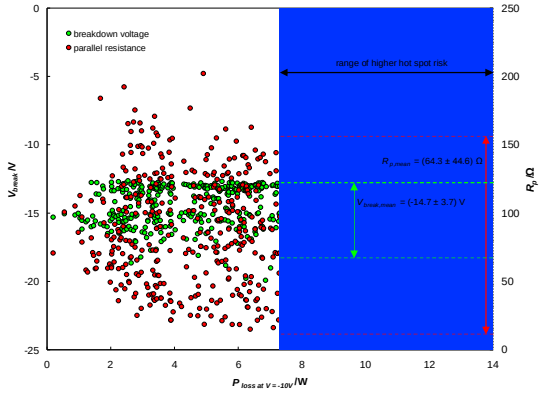

Figure 4: The breakdown voltage and the shunt resistance are vs. dissipated power for 420 different shaded cells.

In Fig.4 a higher dissipation power results in potentially lower breakdown voltages and smaller shunt resistance for the shaded cells. The breakdown voltage V_{break} shows two attraction points at -15 V and -18 V.

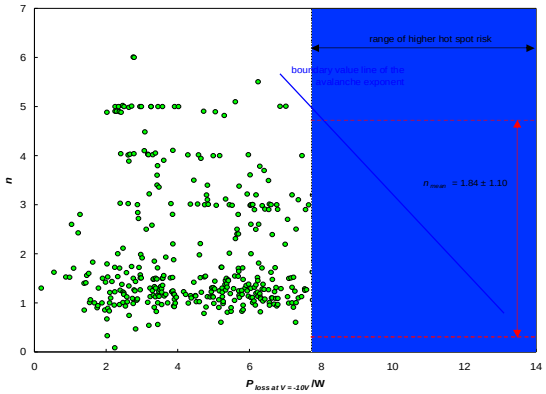

Figure 5: The avalanche exponent n vs. dissipated power for 420 different shaded cells.

In Fig.4 the avalanche exponent is restricted to lower values for higher dissipation powers, i.e. cells with a higher hot spot risk show smaller avalanche exponents. In the range of less risky cells with lower dissipation, the avalanche exponent is confined to n = 1.

Although these parameters are of high practical use for fitting the experimental curves, they show only a weak dependence on the hot spot risk of the shaded cells.

The reason behind is, that the dark reverse current are differently distributed over the individual cell areas. Local currents show more effect on the resulting maximum temperatures, than the total current or total power dissipation in the cell.

3.2 THERMAL ANALYSIS

In this section the result of the (electrical)-thermal investigations are presented. At first the correlation between the hot spot size and the reached maximum temperature under fully shaded conditions of a single cell. The result is showing in figure 6.

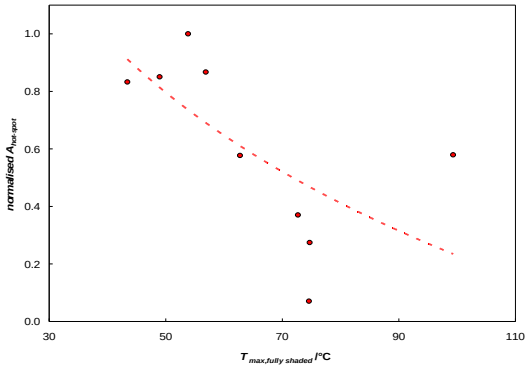

Figure 6: Correlation between the hot spot size and the hot spot temperature.

The trend line in figure 6 displays a relation between the size and the maximum temperature of the hot spot: A decrease of the hot spot size leads to higher maximum temperatures. The reason for this is attributed to a higher leakage current density.

Finally the results of the thermal rapid hot spot analysis are presented. The infrared images are recorded after different irradiation times.

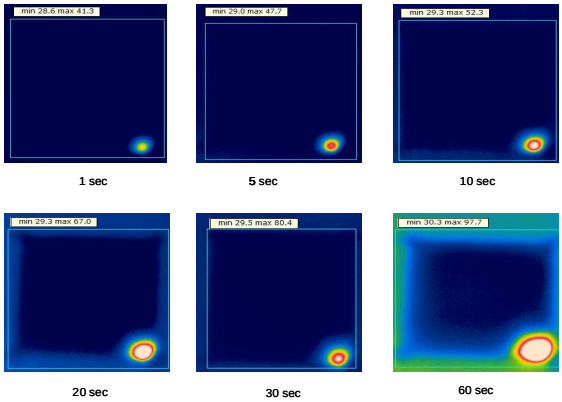

Figure 7: *IR* images of fully shaded single cells at different irradiation times.

As it is displayed the geometry and location of hot spot's becomes apparent after short-time irradiation. Furthermore the temperature and its transient behaviour can be detected.

4 RISK FACTOR COMPARISONS

After describing both methods and presenting its results, their hot spot risk parameters are compared with the measured maximum temperature of a cell after one hour under full shading conditions in Figure 8.

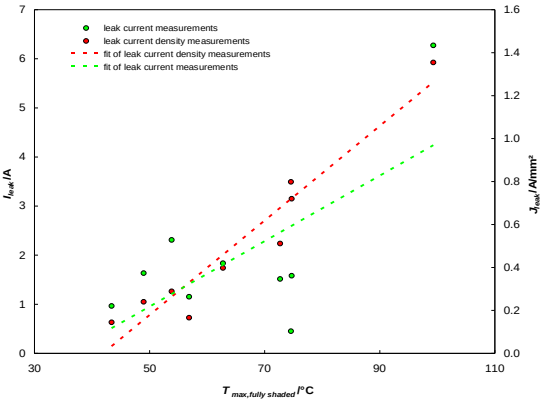

Figure 8: Electrical and thermal hot spot risk factors as the function of the maximum measured temperature.

By plotting the total leakage current and the leakage current density both as a function of the maximum temperature of a fully shaded cell, the leakage current density shows a linear dependence on the maximum temperature. Beside the maximum temperature as a direct hot spot risk parameter, this current density reveals a much better measure for the hot spot risk of the cell and/or the module than the total current.

However, for laboratory use in accordance to the IEC standard, one will still use the total current to determine the worst case cell in the hot spot test procedure.

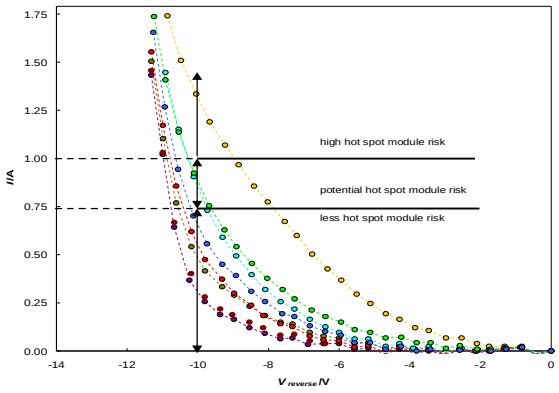

Figure 9: Ranking of critical leakage-currents (for a reverse bias voltage of $V_{reverse}$ = -10 V).

Figure 9 gives indications of the leakage-current at a dark reverse bias voltage of $V_{reverse}$ = -10V. So a cell with a leakage current of $I < 0.75$ A has a less hot spot risk, in the range of $0.75\ A > I > 1.00$ A has a potential risk and a current of $I > 1.00$ A has a high risk. As it is described in this paper, the leakage-current gives no information about the actual temperature rise and the hot spot geometry.

A classification of the hot spot risk in respect to the maximum temperature and corresponding visual features is presented in Table I.

Table I: Critical temperature of the front glass overview

temperature	effect	module consequences
< 150 °C	no visual effects	normal module performance
> 150 °C	melting of encapsulation	delamination and less heat conduction material
> 170 °C	discolouration of the back sheet foil	attenuated of the electrical module isolation
> 200 °C	irreversible destruction of the cell *pn*-junction	performance loss at the module under unshaded conditions

Table 1 indicates that measured front glass temperatures under $T < 150$°C are not critical for modules. Temperatures between $T = 150$°C and $T = 200$°C lead to damaging of synthetic material from the modules. By obtaining temperatures over $T > 200$°C the *pn*-junction becomes destroyed and reduces so the performance of the modules under normal conditions.

5 CONCLUSIONS

The hot spot risk depends on the wafer raw material, the cell process and the cell sorting and string length in the module.

A shaded cell in a module can be distinguished between two types, according to its reverse bias behaviour: current-limited or voltage-limited. The current-limited cells are the less critical. Often, the voltage-limited cells with the highest overall leakage-current show also the highest rise in temperature rise.

Reverse bias *IV* curves can be described by the Bishop model. The hot spot risk factors here are the breakdown voltage, the parallel resistance and the avalanche exponent.

By comparison of these values with the leakage current at the time when the bypass diode turns “on”, it was shown that smaller breakdown voltages and lower parallel resistances correlate with higher dissipated power. The analysis of the hot spot risk using the fitting of the reverse bias curves has to be critically re-considered because that fitting function has four unknown parameters and it relates only weakly to the temperature increase of the shaded cell.

Through short-time illumination (60 sec) of crystalline silicon modules at high irradiances (1000 W/m²) the location, the geometry and the area size of the hot spot can be evaluated from the raw data of an *IR* camera. At hot spots with smaller areas higher temperatures are measured. Hot spots with a smaller area - or a higher leakage current density - are more critical for a hot spot effect in a partially shaded PV module.

ACKNOWLEDGEMENTS

The authors would like to thank the whole Photovoltaik Institut Berlin team, Elkem Solar for allocation of the samples and of course the Reiner Lemoine Foundation for the financial support through a scholarship.

REFERENCES

[1] M.C. Alonso-García et al., "Analysis and modelling the reverse characteristic of photovoltaic cells", Solar Energy Materials & Solar Cells 90 (2006), p. 1105-1120

[2] M.C. Alonso-García et al., "Experimental study of mismatch and shading effects in the I–V characteristic of a photovoltaic module", Solar Energy Materials & Solar Cells 90 (2006), p. 329-340

[3] M. Simon et al., "Detection and analysis of hot-spot formation in solar cells", Solar Energy Materials & Solar Cells 94 (2010), p. 106-113

[4] O. Breitenstein et al., "Understanding junction breakdown in multicrystalline solar cells", Proceedings 20th Workshop on Crystalline Silicon Solar Cells & Modules, p. 1 - 13 NREL, Breckenridge, USA (2010)

[5] W. Kwapil et al., "Investigations on the pre-breakdown of multi-crystalline silicon solar cells", 23rd European Photovoltaic Solar Energy Conference, 1 - 5 September 2008, Valencia, Spain

[6] A. Bodycombe et al., "Thermal and Electrical effects of partial shading on photovoltaic modules", CREST, Loughborough University, September 1997

[7] J. Wohlgemuth, W. Herrmann, "Hot spot tests for crystalline silicon modules" Photovoltaic Specialists Conference, 31st IEEE (2005), p. 1062

[8] S. Pingel et al., "Potential Induced Degradation of solar cells and panels", 35th IEEE Photovoltaic Specialists Conference, Honolulu, Hawaii, USA 2010

[9] W. Herrmann et al., "Hot spot investigations on PV modules - new concepts for a test standard and consequences for module design with respect to bypass diodes", 26th IEEE Photovoltaic Specialists Conference, Anaheim (1997), p. 1129-1132

[10] J. W. Bishop, "Computer simulation of the effects of electrical mismatches in photovoltaic cell interconnection circuits", Solar Cells 25 (1988), p. 73 - 89